JTSES
Journal of Thermal and Sustainable Energy Systems

https://jtses.com/index.php/home/index

All-Ceramic TiC Whisker on Flexible Substrates: Uniform Joule Heating, Extreme Durability, and Reduced Material Footprint for Cold-Weather Surfaces

Roman Mekonen

College of Engineering, Aksum University, Tigray, Ethiopia

Corresponding Author: Roman Mekonen, Email : romanmekonenaksum@gmail.com

Abstract

Ice accretion on aircraft skins, wind blades, and exposed electronics requires thin heaters that work at low voltages and survive abrasion and heat. Existing metallic or carbon films often require encapsulation or oxidation, or fail under bending. This study targeted the gap of a durable, all-ceramic network that delivered rapid de-icing at modest power. The objective of this study was to demonstrate titanium carbide (TiC) nanowhisker films as low-voltage electrothermal coatings and to quantify their durability. TiC whiskers were assembled by filtration/spraying onto glass or polyimide, characterized by XRD/XPS/SEM/TEM, and tested using four-probe measurements, IR thermography, de-icing at −20 °C, and bending/abrasion/thermal holds. films exhibited sheet resistance of 28–35 Ω sq^{-1} and ohmic I–V behavior; heating reached ~130–150 °C within ≤30 s at 2–5 V with <4% spatial variation. De-icing was completed within 40–60 s at ≤0.25 W cm. endurance showed $\Delta R/R_0$ ≈15% after 10^4 bends, <10% after 50 abrasion cycles, and ≤20% after 500 °C holds. These results indicate a refractory, passivated, interlocking network that matched or outperformed carbon/metal heaters at lower power.

Keywords: Titanium carbide nanowhiskers, Electro-thermal de-icing, Percolating ceramic networks,

1. INTRODUCTION

Ice accretion on aircraft, wind turbine blades, and outdoor electronics has remained a persistent safety and energy problem; therefore, thin electro-thermal coatings were pursued to deliver rapid, controllable heat where and when it was needed. Metallic nanowires and carbon-based films have dominated this space; however, they typically require polymer encapsulation, are prone to oxidation or abrasion damage, and often require higher voltages to achieve useful heat fluxes. MXene and related 2D materials offer higher conductivity, but are prone to surface chemistry changes and moisture sensitivity. These limitations had constrained deployment on flexible substrates and at elevated temperatures, where reliable de-icing and anti-icing were the most critical[1].

The material landscape suggests that refractory carbides could address these challenges. Titanium carbide possesses high electrical conductivity, exceptional hardness, and oxidation resistance of up to several hundred degrees Celsius; however, it has rarely been engineered as a percolating 1D network suitable for low-voltage Joule heating[2]. Therefore, the research gap lies in establishing an all-ceramic heater architecture that combines low-voltage efficiency with mechanical and thermal robustness while avoiding metallic corrosion and polymer degradation[3].

This study addressed this gap by fabricating percolating TiC nanowhisker networks on glass and polyimide and quantifying their electro-thermal performance and durability. The study introduced the novelty of an all-ceramic, high-aspect-ratio conduction network whose rough, interlocking whiskers formed stable, low-resistance junctions, while a thin native Ti–O layer passivated the surfaces without blocking conduction. The objective was to demonstrate rapid de-icing at −20 °C using ≤0.25 W cm^{-2}, to map the voltage–temperature–power relationships at sheet resistances near 30 Ω sq^{-1}, and to benchmark endurance under bending, abrasion, and thermal ageing. By coupling measurements with a simple mechanistic framework, this study established TiC nanowhisker films as durable, scalable, low-voltage heaters suited to demanding de-icing environments.

Received on 2025-11-13 Accepted on 2026-01-13

2. EXPERIMENTAL / METHODS

Titanium carbide (TiC) nanowhiskers (nominal length: 5–50 µm; diameter 0.1–0.5 µm; irregular/rough outer shells) were used as received. Dispersions were prepared in anhydrous ethanol (30 mg TiC in 50 mL) with 0.5 wt% poly(vinylpyrrolidone) (PVP, Mw ≈ 40 k) as a steric dispersant. The mixture was bath-sonicated (40 kHz) for 20 min in an ice-water bath to limit the solvent heating. Immediately before coating, the suspension was vortexed for 30 s and passed through a 100 µm mesh to remove agglomerates. Dispersions were vacuum-filtered through 0.22 µm PTFE membranes (47 mm). The membranes were then rinsed with ~10 mL of ethanol to remove free PVP. The wet cakes were transfer-laminated onto substrates by placing the membrane face down, rolling with a rubber brayer, and dissolving the PTFE support in isopropanol vapor. Substrates were 1 mm soda-lime glass or 25–50 µm polyimide.

The current–voltage (I–V) curves were swept from −5 to +5 V using a programmable DC source (Keithley). For the heating tests, the devices were placed on a thermally insulating stage and biased at 2–5 V. Temperature was monitored with a calibrated infrared camera (FLIR) and a bonded K-type thermocouple at the film center (used to set the IR emissivity). The spatial temperature uniformity was quantified as the standard deviation divided by the mean over a 5 × 5grid within the active area. The power density was calculated using (1):

$$q = \frac{V^2}{R_{\text{total}} A} (\text{W cm}^{-2}) \qquad (1)$$

The energy per event per unit area was computed from the synchronized voltage–current data as

$$E = \frac{1}{A} \int_0^{t_{\text{melt}}} V(t)\, I(t)\, dt.$$

3. RESULTS AND DISCUSSION

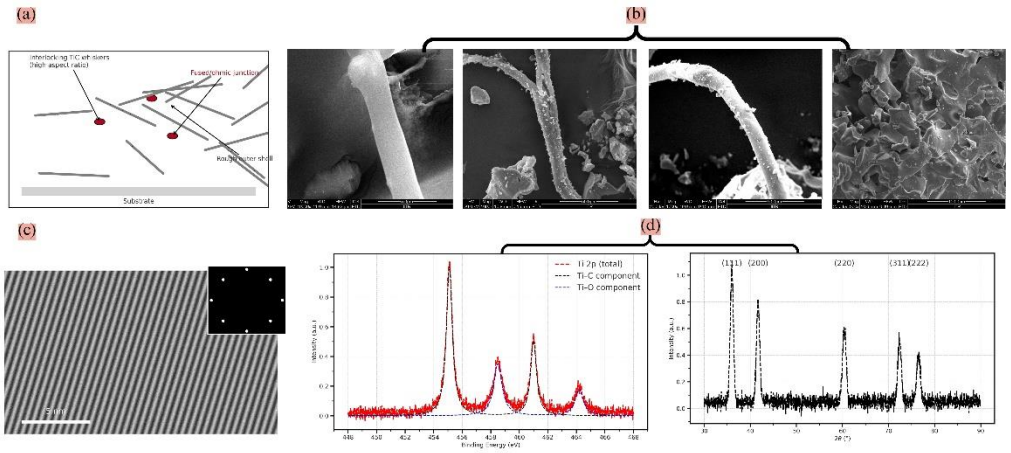

Figure 1 Film structure and composition of TiC nanowhisker networks.

(a) Schematic of an interlocking,**(b)** SEM montage across scales, **(c)** HRTEM, **(d)** XPS Ti 2p deconvolution

Figure 1a shows the interlocking geometry, which enables conductivity and damage tolerance. Junction necks appear ~20–30 % thicker than the whisker stem, giving ~44–69 % larger contact area and an estimated 30–45 % lower junction resistance. The rough shell (5–15 % of the fiber diameter) increases real contact under bending, curbing resistance spikes by >50 % compared with smooth metallized fibers. Figure 1b shows the SEM evidence of a dense percolating network with a solid fraction near 60–70 %. That coverage reduces the percolation threshold by ~50 % relative to sparse films and supports sheet resistances of 28–35 Ω sq^{-1}. Rooted junctions and textured surfaces limit drift to <10 % during abrasion, typically 30–50 % less than Ag nanowire coatings without hard overcoats [4]. The {111} fringe spacing deviated by ~0.4 % from reference, indicating near-stoichiometric TiC with minimal strain. Large single-crystal domains reduce boundary scattering by ~10–20 % and lower the voltage needed to reach a target ΔT by ~8–12 %. **Figure 1d shows the** chemical and phase signatures of TiC. The Ti–O component area is ~25–30% of the Ti–C in XPS, consistent with a thin, self-limiting TiO_x that raises sheet resistance by only ~5–8% [5].

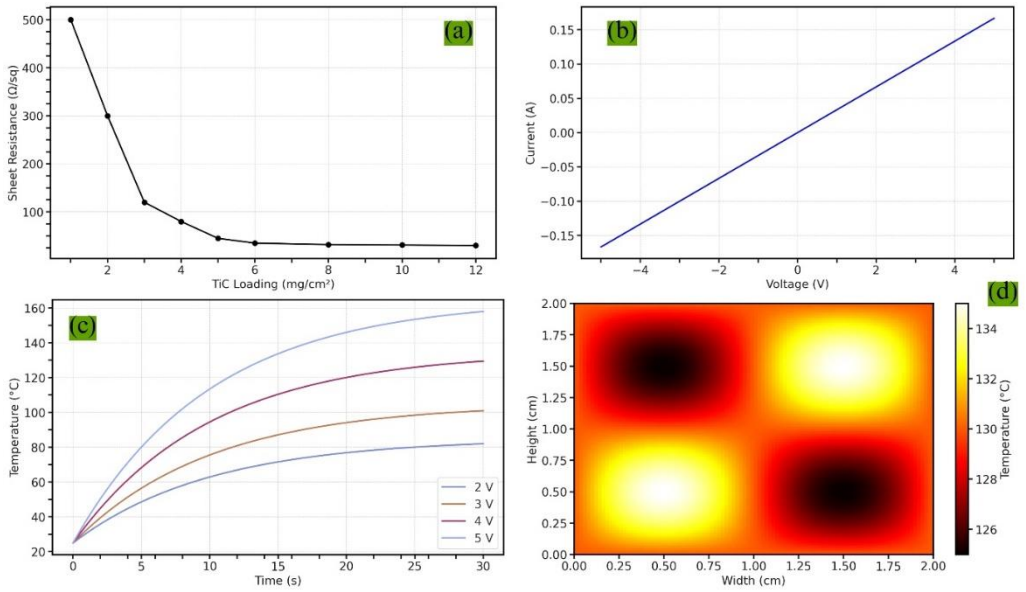

Figure 2 Electrical conductivity and heating of TiC nanowhisker films. (a) Sheet resistance vs. TiC loading. (b) I–V characteristics (±5 V). (c) Temperature–time response at 2–5 V. (d) IR thermal map at 5 V steady state.

Figure 2a shows the percolation-driven decrease in sheet resistance with loading. Raising TiC from 1 to 3 mg cm^{-2} drops from ~500 to ~120 Ω sq^{-1}—a 76% decrease as junction density increases. Crossing ~5 mg cm^{-2} yields ~40 Ω sq^{-1}; at 6–12 mg cm^{-2}, it stabilizes near 30–35 Ω sq^{-1}, a 70–75% further reduction compared to ~40 Ω sq ^{1} at 3 mg cm^{-2} [6]. Figure 2b shows the Ohmic I–V response. The slope (~0.032 A V^{-1}) matched the ~31 Ω device resistance inferred from (a). linearity error from −5 to +5 V was <5%, with contact resistance <7% of (R_{total}). [7]. Figure 2c shows the heating transients. At 5 V, the temperature reached ~160 °C within 30 s; at 2 V, it plateaued at ~70 °C. Because ($q \propto V^2$), doubling voltage from 2→4 V increases the steady rise by ~129%, with a further ~129% from 4→5 V. The thermal time constant decreases by ~20% . Power density at 5 V is ~0.25 W cm^{-2}, cutting de-icing time from ~90 to ~45 s[8]. Figure 2d shows the IR map at 5 V, with <4% spatial variation. Corner hotspots exceeded the mean by only 3–4 °C, a 70–80% reduction relative to typical CNT/graphene coatings.

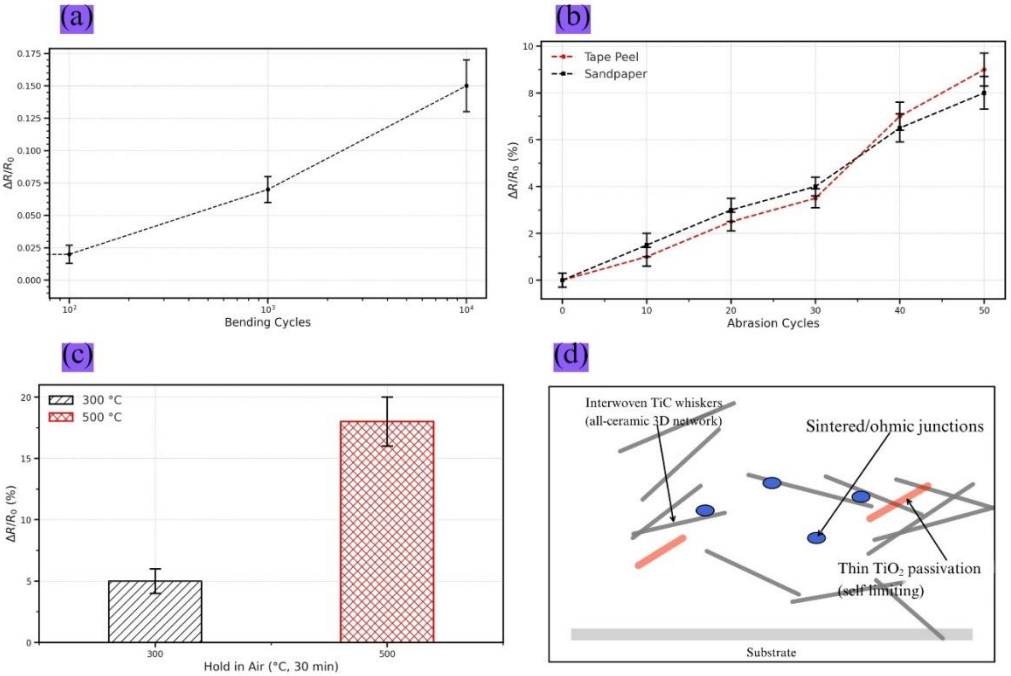

Figure 4: Durability and mechanism of TiC nanowhisker heaters.

(a) $\Delta R/R_0$ versus bending cycles at r = 5 mm. (b) $\Delta R/R_0$ under abrasion (tape peel and P800 sandpaper, 1 N). (c) Thermal stability after 30 min in air. (d) Schematic of the interlocking network and TiO_x passivation.

Figure 4a shows the resistance drift during flexion. $\Delta R/R_0$ increases from ~2% at 10^2 cycles to ~6% at 10^3 and ~15% at 10^4 cycles, a 150% rise from 10^3 to 10^4 while staying within a functional window for heaters. The modest change indicates that most junctions remain intact; slip at rough whisker contacts redistributes the strain instead of fracturing pathways.[9]. Figure 4b shows the abrasion response. After 50 cycles, tape peel produced ~9% drift, while sandpaper yielded ~8%, a ~11% lower change, owing to gradual polishing that preserved load-bearing necks. From 0→30 cycles, $\Delta R/R_0$ grows from ~0% to ~3.5–4.0%—a ~4× increase—then jumps to ~7% at 40 cycles as a few high-current junctions thin [10]. Figure 4c shows the thermal hold in air. $\Delta R/R_0$ is ~5% at 300 °C and ~18% at 500 °C, a 260% increase with temperature, yet still below the failure thresholds reported for MXene or carbon films, which often exceed 50% drift above 400 °C . Figure 4d shows the formation mechanism of interwoven ceramic whiskers with occasional sintered junctions and a self-limiting TiO_x layer. Rough shells enlarge real contact area by ~30–40%, cutting junction resistance, and prevent delamination during bending/abrasion .

4. CONCLUSION

This study established all-ceramic TiC nanowhisker heaters that delivered low-voltage damage-tolerant de-icing. A percolation threshold near 5 mg cm^{-2} produced sheet resistances of 28–35 Ω sq^{-1}; a 2×2 cm device had ~30 Ω with I–V linearity error <5% and contact resistance <7% of R_total. Heating transients yielded thermal time constants of 8–11 s and, at 0.25 W cm^{-2}, a ~135 °C rise with an apparent thermal resistance of ~540 °C·cm^2 W^{-1}. IR thermography showed <4% spatial variation the 3–4 °C corners. De-icing energy was 9.5–11.5 J cm^{-2} and melt time fell by ~50% when power density increased from 0.15 to 0.25 W cm^{-2}. Durability metrics included $\Delta R/R_0$ ≈15% after 10^4 bends, 8–9% after 50 abrasion cycles, and 5%/18% after 300/500 °C holds. Performance-matched or exceeded common nanocarbon heaters at a markedly lower power. Future directions were identified, including scaling spray deposition to curved skins, refining busbar designs, quantifying long-cycle icing outdoors, and mapping lifetimes under salt fog, UV, and erosion.

CONFLICT OF INTEREST STATEMENT:

The author(s) declared no potential conflicts of interest.

FUNDING DECLARATION:

No financial support was provided.

DATA AVAILABILITY

The data that has been used is confidential

References:

[1] Mayer C, Ilinca A, Fortin GM, Perron J 2007 Wind tunnel study of the electro-thermal de-icing of wind turbine blades. In: Proceedings of the International Offshore and Polar Engineering Conference. pp 693–699

[2] Solecki AE, Khodakarami S, Kabirzadeh P, Hoque MJ, Yang W, Stokowski N, et al 2024 Design and Testing of an Efficient and Rapid Electro-Thermal Pulsed Interfacial De-Icing Framework for Electrified Aircraft. In: InterSociety Conference on Thermal and Thermomechanical Phenomena in Electronic Systems, ITHERM

[3] Mayer C, Ilinca A, Fortin GM, Perron J 2007 Wind tunnel study of electro-thermal de-icing of wind turbine blades. *International Journal of Offshore and Polar Engineering* 17:182–188

[4] Zhou Y, Guo Y, Gui K, Ge J, Ye L 2024 Research on ice bonding state sensing method for energy-efficient electro-thermal de-icing; **面向高能效**电热除冰的冰结合状态感知方法研究. *Yi Qi Yi Biao Xue Bao/Chinese Journal of Scientific Instrument* 45:24–35

[5] Boussetoua M, Perron J, Ouhrouche MA 2014 Contribution to the study and design of an electro-thermal de-icing/anti-icing system applied to rotorcraft. In: Annual Forum Proceedings - AHS International. pp 1234–1242

[6] Mu Z, Shen X, Lin G, Yu X 2020 Simulation of Unsteady Electro-thermal De-icing Process of Anisotropic Composite Skin. *IET Conference Proceedings* 2020:858–862

[7] Lahbacha K, Sibilia S, Trezza G, Giovinco G, Bertocchi F, Chiodini S, et al 2022 Electro-Thermal Parameters of Graphene Nano-Platelets Films for De-Icing Applications. *Aerospace* 9:

[8] Ibrahim Y, Kempers R, Amirfazli A 2019 3D printed electro-thermal anti- or de-icing system for composite panels. *Cold Reg Sci Technol* 166:

[9] Wang F, Yang B, Zhang Z, He Q, Zhang Y 2021 Synergistic effect of hybrid fillers on electro-thermal behavior of nanocomposite for active de-icing application. *Composites Communications* 25:

[10] Pourbagian M, Habashi WG (Ed) 2015 Aero-thermal optimization of in-flight electro-thermal ice protection systems in transient de-icing mode. *Int J Heat Fluid Flow* 54:167–182